Engineering Transactions, **67**(4): 491–512, 2019, doi: 10.24423/EngTrans.1015.20190725
Polish Academy of Sciences • Institute of Fundamental Technological Research (IPPT PAN)
Université de Lorraine • Poznan University of Technology

Research Paper

Analytical and Numerical Studies of an Unsymmetrical Sandwich Beam – Bending, Buckling and Free Vibration

Krzysztof MAGNUCKI[1)], Ewa MAGNUCKA-BLANDZI[2)]
Jerzy LEWIŃSKI[1)*], Szymon MILECKI[1)]

[1)] *Institute of Rail Vehicles TABOR*
Warszawska 181, 61-055 Poznan, Poland
*Corresponding Author e-mail: jerzy.lewinski@tabor.com.pl

[2)] *Institute of Mathematics*
Poznan University of Technology
Piotrowo 3A, 60-965 Poznan, Poland

The subject of the paper is an unsymmetrical sandwich beam. The thicknesses and mechanical properties of the beam faces are different. Mathematical model of the beam is formulated based on the classical broken-line hypothesis. The equations of motions of the beam is derived on the ground of the Hamilton's principle. Bending, buckling and free-vibration are studied in detail for exemplary unsymmetrical structure of the beam. The values of deflection, critical force and natural frequency are determined for the selected beam cases. Moreover, the same examples are computed with the use of two FEM systems, i.e. SolidWorks and ABAQUS, in order to compare the analytical and numerical calculation. The results are presented in tables and figures.

Key words: sandwich beams; beam deflection; critical load; free vibration; analytical studies; FEM studies.

1. Introduction

The theory and application of the sandwich structures have been initiated in the mid of 20th century. Vinson [1] presented a review of the most important papers of the 20th century, related to the sandwich structures. Carrera [2] delivered a historical overview of the theories developed in order to analyse the multilayered structures, with special attention paid to the Zig-Zag hypothesis. Frostig and Shenhar [3] analysed bending of the sandwich beam of unsymmetrical structure. Icardi [4] presented a sublaminate model determined to analyse the laminated and sandwich beams, using a general zig-zag approximation. Kim and Swanson [5] studied the sandwich beams with fibre com-

posite faces and polymeric foam cores. BACKSTÖM and NILSSON [6] considered possible use of modified lower order methods (the Bernoulli-Euler and Timoshenko beam theories) to calculate the response of asymmetric sandwich beams under various boundary conditions. MAGNUCKA-BLANDZI and MAGNUCKI [7] presented the effective design of sandwich beams with symmetrically varying mechanical properties of the cores. MAGNUCKA-BLANDZI [8] described static and dynamic stability of sandwich beams with a metal foam core, using three hypotheses of the cross section deformation. WANG and LI [9] presented the theoretical analysis of the deformation of Shape Memory Polymers sandwich beam in flexural state. BABA [10] presented experimental and numerical studies of natural frequencies of flat and curved beams. ELTAHER *et al.* [11] studied bending and natural frequencies of the functionally graded beams, with consideration of location of the beam neutral axis. JASION and MAGNUCKI [12] presented theoretical studies on global buckling of a sandwich column with nonlinear mechanical properties of metal foam core. MAGNUCKI *et al.* [13] developed a mathematical model of a five-layer beam of symmetrical structure. WU *et al.* [14] solved the buckling and free vibration problems of a sandwich beam of symmetrical structure. FILIPPI and CARRERA [15] proposed the theories using higher-order Zig-Zag functions defined over the cross-section layers. FROSTIG [16] analytically described the buckling problem of sandwich plates with consideration of the shear effect, and solved it for exemplary structures. KIM and LEE [17] presented a geometrically nonlinear study of functionally graded plates, with consideration of the neutral surface position. CHEN *et al.* [18] presented analytical models of symmetrical and unsymmetrical structures of sandwich beams with porous cores. MAGNUCKA-BLANDZI and RODAK [19] devoted their paper to a metal seven-layer beam, composed of a plate band with a lengthwise trapezoidal corrugation considered as a main core and two crosswise trapezoidally corrugated cores considered as the faces. MAGNUCKA-BLANDZI [20] studied a thin-walled simply supported sandwich beam composed of seven layers. The facings of the beam are of three-layer structure and are separated by a main core being a trapezoidally crosswise corrugated layer. SAYYAD and GHUGAL [21] presented an extensive critical review of the literature devoted to bending, buckling vibration of laminated and sandwich beams based on the single layer theories, layerwise theories, zig-zag theories and exact solutions. YANG *et al.* [22] provided analytical solutions of free vibration of the laminate, box and sandwich beams. VO *et al.* [23] dealt with bending of laminated composite and sandwich beams using a quasi-3D theory, with consideration of normal and shear deformation effects. ZHEN *et al.* [24] proposed a Reddy-type higher-order Zig-Zag theory. SAYYAD and GHUGAL [25] provided a review of research studies devoted to modeling and analysis of functionally graded sandwich beams. MAGNUCKI [26] presented an analytical modelling of sandwich beams

and I-beams with the use of the classical "broken line" hypothesis and nonlinear hypothesis.

The subject of the study is a simply supported unsymmetrical sandwich beam of length L and width b. The beam is under uniformly distributed transverse load of intensity q or under axial compression force F_0. Faces of the beam are of different thicknesses t_{f1}, t_{f2} and are made of different materials with Young's modules E_{f1}, E_{f2} and mass densities ρ_{f1}, ρ_{f2}. The core of thickness t_c is made of material with elastic modules E_c, G_c, Poisson ratio ν_c and mass density ρ_c (Fig. 1).

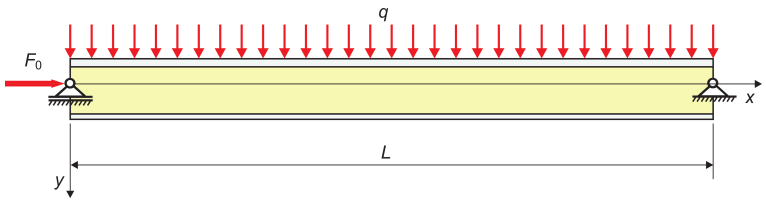

FIG. 1. Scheme of the unsymmetrical sandwich beam and load.

The xy coordinate system is assumed as is shown in Fig. 2. The neutral axis is collinear with the x axis. Due to unsymmetrical structure of the beam the neutral axis is shifted by y_0 with regard to geometrical symmetry axis of the core. The problem of the neutral axis position was noticed by many authors, e.g. FROSTIG and SHENHAR [3], ELTAHER *et al.* [11], KIM and LEE [17]. The authors of the above papers determined the position of the neutral axis in an approximate way.

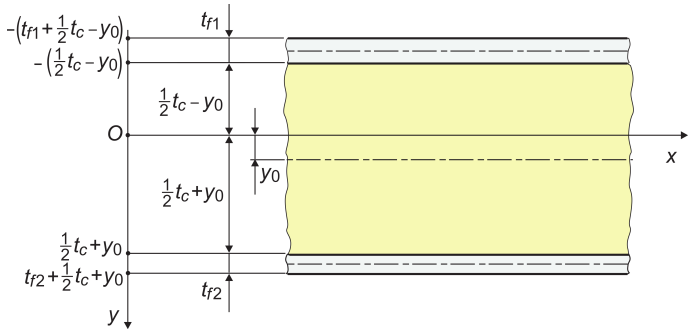

FIG. 2. Dimensions of the beam and the coordinate system xy.

In the present paper the problem of the neutral axis location is solved with two methods. In the first approach the neutral axis is determined based on zeroing of the longitudinal normal force, while in the other it is obtained from maximization of maximum deflection, minimization of critical load or free vi-

bration frequency, in accordance with the Hamilton's principle. The results of deflection, critical load and free vibration frequency obtained from analytical approach are compared to the ones computed with the Finite Element Method.

2. Analytical model of the beam

The classical broken line hypothesis is assumed for modelling of the beam. In result of deformation of the plane cross section the straight line before bending transforms into a broken line (Fig. 3).

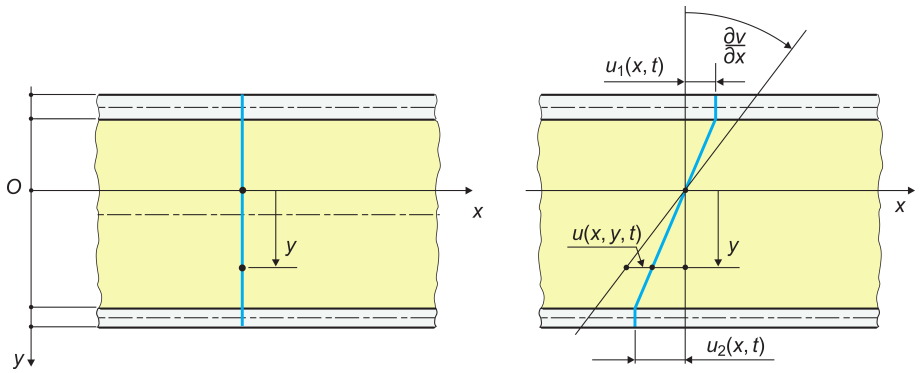

Fig. 3. The deformation of plane cross section of the beam – the broken line hypothesis.

Displacements in the subsequent layers of the beam with consideration of the hypothesis (Fig. 3) are as follows

- the upper face $-\left(x_{f1}+\frac{1}{2}-\eta_0\right) \le \eta \le -\left(\frac{1}{2}-\eta_0\right)$

$$u(x,y,t) = -\left[y\frac{\partial v}{\partial x} - u_1(x,t)\right] = -t_c\left[\eta\frac{\partial v}{\partial x} + \left(\frac{1}{2}-\eta_0\right)\psi_0(x,t)\right], \tag{2.1}$$

- the core $-\left(\frac{1}{2}-\eta_0\right) \le \eta \le \frac{1}{2}+\eta_0$

$$u(x,y,t) = -y\left[\frac{\partial v}{\partial x} - \psi_0(x,t)\right] = -t_c\eta\left[\frac{\partial v}{\partial x} - \psi_0(x,t)\right], \tag{2.2}$$

- the lower face $\frac{1}{2}+\eta_0 \le \eta \le x_{f2}+\frac{1}{2}+\eta_0$

$$u(x,y,t) = -y\frac{\partial v}{\partial x} + u_2(x,t) = -t_c\left[\eta\frac{\partial v}{\partial x} - \left(\frac{1}{2}+\eta_0\right)\psi_0(x,t)\right], \tag{2.3}$$

where $v(x,t)$ – deflection, $\eta = y/t_c$ – dimensionless coordinate, $\eta_0 = y_0/t_c$, $x_{f1} = t_{f1}/t_c$, $x_{f2} = t_{f2}/t_c$ – dimensionless parameters, $\psi_0(x,t)$ – dimensionless function of the shear effect.

The displacements in the upper and lower faces, considering the dimensionless function of the shear effect, are:

$$u_1(x,t) = t_c\left(\frac{1}{2} - \eta_0\right)\psi_0(x,t), \qquad u_2(x,t) = t_c\left(\frac{1}{2} + \eta_0\right)\psi_0(x,t). \tag{2.4}$$

Therefore, longitudinal and shear strains in the subsequent layers of the beam are as follows:

- the upper face

$$\varepsilon_x^{(u-f)} = \frac{\partial u}{\partial x} = -t_c\left[\eta\frac{\partial^2 v}{\partial x^2} + \left(\frac{1}{2} - \eta_0\right)\frac{\partial \psi_0}{\partial x}\right], \qquad \gamma_{xy}^{(u-f)} = \frac{\partial u}{\partial y} + \frac{\partial v}{\partial x} = 0, \tag{2.5}$$

- the core

$$\varepsilon_x^{(c)} = \frac{\partial u}{\partial x} = -t_c\eta\left[\frac{\partial^2 v}{\partial x^2} - \frac{\partial \psi_0}{\partial x}\right], \qquad \gamma_{xy}^{(c)} = \frac{\partial u}{\partial y} + \frac{\partial v}{\partial x} = \psi_0(x,t), \tag{2.6}$$

- the lower face

$$\varepsilon_x^{(l-f)} = \frac{\partial u}{\partial x} = -t_c\left[\eta\frac{\partial^2 v}{\partial x^2} - \left(\frac{1}{2} + \eta_0\right)\frac{\partial \psi_0}{\partial x}\right], \qquad \gamma_{xy}^{(l-f)} = \frac{\partial u}{\partial y} + \frac{\partial v}{\partial x} = 0. \tag{2.7}$$

The stresses (Hooke's law) for these layers:

$$\sigma_x^{(u-f)} = E_{f1}\varepsilon_x^{(u-f)}, \qquad \tau_{xy}^{(u-f)} = 0, \tag{2.8}$$

$$\sigma_x^{(c)} = E_c\varepsilon_x^{(c)}, \qquad \tau_{xy}^{(c)} = G_c\gamma_{xy}^{(c)}, \tag{2.9}$$

$$\sigma_x^{(l-f)} = E_{f1}\varepsilon_x^{(u-f)}, \qquad \tau_{xy}^{(l-f)} = 0. \tag{2.10}$$

The kinetic energy of the beam

$$T = \frac{1}{2}bt_c\rho_b\int_0^L\left(\frac{\partial v}{\partial t}\right)^2 \mathrm{d}x, \tag{2.11}$$

where t – time, $\rho_b = x_{f1}\rho_{f1} + \rho_c + x_{f2}\rho_{f2}$ – mass density of the beam.

The elastic strain energy of the beam

$$U_\varepsilon = U_\varepsilon^{(u-f)} + U_\varepsilon^{(c)} + U_\varepsilon^{(l-f)}, \tag{2.12}$$

where

- elastic strain energy of the upper face:

$$U_{\varepsilon}^{(u-f)} = \frac{1}{2} E_{f1} b t_c \int_0^L \int_{-\left(x_{f1}+\frac{1}{2}-\eta_0\right)}^{-\left(\frac{1}{2}-\eta_0\right)} \left[\varepsilon_x^{(u-f)}\right]^2 \mathrm{d}\eta \, \mathrm{d}x,$$

- elastic strain energy of the core:

$$U_{\varepsilon}^{(c)} = \frac{1}{2} b t_c \int_0^L \int_{-\left(\frac{1}{2}-\eta_0\right)}^{\frac{1}{2}+\eta_0} \left\{ E_c \left[\varepsilon_x^{(c)}\right]^2 + G_c \frac{\left(\psi_0(x,t)\right)^2}{t_c^2} \right\} \mathrm{d}\eta \, \mathrm{d}x,$$

- elastic strain energy of the lower face:

$$U_{\varepsilon}^{(l-f)} = \frac{1}{2} E_{f2} b t_c \int_0^L \int_{\frac{1}{2}+\eta_0}^{x_{f2}+\frac{1}{2}+\eta_0} \left[\varepsilon_x^{(l-f)}\right]^2 \mathrm{d}\eta \, \mathrm{d}x.$$

The work of the load

$$W = \int_0^L \left[q v(x) + \frac{1}{2} F_0 \left(\frac{\partial v}{\partial x} \right)^2 \right] \mathrm{d}x, \tag{2.13}$$

where q – intensity of the transverse load, F_0 – axial compression force (Fig. 1).

Based on the Hamilton's principle

$$\delta \int_{t_1}^{t_2} \left[T - (U_{\varepsilon} - W) \right] \mathrm{d}t = 0, \tag{2.14}$$

with consideration of the expressions (2.5)–(2.7) for the strains in elastic strain energy (2.12) and integrating on the depth of the beam, two differential equations of motion are obtained

$$b t_c \rho_b \frac{\partial^2 v}{\partial t^2} + b t_c^3 \left(C_{vv} \frac{\partial^4 v}{\partial x^4} - C_{v\psi_0} \frac{\partial^3 \psi_0}{\partial x^3} \right) + F_0 \frac{\partial^2 v}{\partial x^2} = q, \tag{2.15}$$

$$C_{v\psi_0} \frac{\partial^3 v}{\partial x^3} - C_{\psi_0\psi_0} \frac{\partial^2 \psi_0}{\partial x^2} + G_c \frac{\psi_0(x,t)}{t_c^2} = 0, \tag{2.16}$$

where

$$C_{vv} = \frac{1}{12} \left[E_{f1} x_{f1} \varphi_1 + E_c \left(1 + 12\eta_0^2\right) + E_{f2} x_{f2} \varphi_2 \right],$$

$$C_{v\psi_0} = \frac{1}{4}\left[E_{f1}x_{f1}\varphi_3 + \frac{1}{3}E_c\left(1+12\eta_0^2\right) + E_{f2}x_{f2}\varphi_4\right],$$

$$\varphi_1 = 4x_{f1}^2 + 6x_{f1}\left(1-2\eta_0\right) + 3\left(1-2\eta_0\right)^2,$$

$$\varphi_2 = 4x_{f2}^2 + 6x_{f2}\left(1+2\eta_0\right) + 3\left(1+2\eta_0\right)^2,$$

$$\varphi_3 = \left(x_{f1}+1-2\eta_0\right)\left(1-2\eta_0\right),$$

$$\varphi_4 = \left(x_{f2}+1+2\eta_0\right)\left(1+2\eta_0\right),$$

$$C_{\psi_0\psi_0} = \frac{1}{4}\left[E_{f1}x_{f1}\left(1-2\eta_0\right)^2 + \frac{1}{3}E_c\left(1+12\eta_0^2\right) + E_{f2}x_{f2}\left(1+2\eta_0\right)^2\right].$$

The bending moment

$$M_b(x,t) = -bt_c^3\left\{E_{f1}\int\limits_{-\left(x_{f1}+\frac{1}{2}-\eta_0\right)}^{-\left(\frac{1}{2}-\eta_0\right)}\eta\varepsilon_x^{(u-f)}\,\mathrm{d}\eta + E_c\int\limits_{-\left(\frac{1}{2}-\eta_0\right)}^{\frac{1}{2}+\eta_0}\eta\varepsilon_x^{(c)}\,\mathrm{d}\eta + E_{f2}\int\limits_{\frac{1}{2}+\eta_0}^{x_{f2}+\frac{1}{2}+\eta_0}\eta\varepsilon_x^{(l-f)}\,\mathrm{d}\eta\right\}. \tag{2.17}$$

Substituting the expressions (2.5)–(2.7) for the longitudinal strains and integrating on the depth of the beam, one obtains the following equation

$$C_{vv}\frac{\partial^2 v}{\partial x^2} - C_{v\psi_0}\frac{\partial\psi_0}{\partial x} = -\frac{M_b(x,t)}{bt_c^3}. \tag{2.18}$$

This equation is equivalent to the equation (2.15) for static problems.

The axial force

$$N(x,t) = -bt_c^3\left\{E_{f1}\int\limits_{-\left(x_{f1}+\frac{1}{2}-\eta_0\right)}^{-\left(\frac{1}{2}-\eta_0\right)}\varepsilon_x^{(u-f)}\,\mathrm{d}\eta + E_c\int\limits_{-\left(\frac{1}{2}-\eta_0\right)}^{\frac{1}{2}+\eta_0}\varepsilon_x^{(c)}\,\mathrm{d}\eta + E_{f2}\int\limits_{\frac{1}{2}+\eta_0}^{x_{f2}+\frac{1}{2}+\eta_0}\varepsilon_x^{(l-f)}\,\mathrm{d}\eta\right\} = 0. \tag{2.19}$$

Substituting the expressions (2.5)–(2.7) for the longitudinal strains and integrating on the depth of the beam, one obtains the condition allowing to calculate the position of neutral axis – dimensionless parameter η_0, in the following form

$$C_{Nv}\frac{\partial^2 v}{\partial x^2} - C_{N\psi_0}\frac{\partial \psi_0}{\partial x} = 0, \tag{2.20}$$

where

$$C_{Nv} = \frac{1}{2}E_{f1}x_{f1}\left(x_{f1} + 1 - 2\eta_0\right) - E_c\eta_0 - \frac{1}{2}E_{f2}x_{f2}\left(x_{f2} + 1 + 2\eta_0\right),$$

$$C_{N\psi_0} = \frac{1}{2}E_{f1}x_{f1}\left(1 - 2\eta_0\right) - E_c\eta_0 - \frac{1}{2}E_{f2}x_{f2}\left(1 + 2\eta_0\right).$$

Disregarding the effect of shear on the position of the neutral axis (Fig. 2) in order to simplify the approach, the condition (2.20) reduces itself to $C_{Nv} = 0$, from which

$$\eta_0 = \frac{E_{f1}x_{f1}\left(1 + x_{f1}\right) - E_{f2}x_{f2}\left(1 + x_{f2}\right)}{2\left(E_{f1}x_{f1} + E_c + E_{f2}x_{f2}\right)}. \tag{2.21}$$

Moreover, it should be noticed, that the position of the neutral axis results from the theorem of minimum potential energy. Therefore, the maximal deflection of the simply supported beam

$$v_{\max} = \max_{\eta_0}\left\{v\left(\frac{L}{2}, \eta_0\right)\right\}, \tag{2.22}$$

and, similarly, the critical force and fundamental natural frequency

$$F_{0,CR} = \min_{\eta_0}\left\{F_0\left(\eta_0\right)\right\}, \qquad \omega = \min_{\eta_0}\left\{\omega\left(\eta_0\right)\right\}. \tag{2.23}$$

3. Analytical study of the problems

3.1. Bending of the beam – static problem

The bending moment of the beam under uniformly distributed transverse load of intensity q (Fig. 1) is $M_b(x) = q(L-x)x/2$. Therefore, the system of two equations of equilibrium (2.18) and (2.16) is in the following form

$$\begin{aligned} C_{vv}\frac{\mathrm{d}^2 v}{\mathrm{d}x^2} - C_{v\psi_0}\frac{\mathrm{d}\psi_0}{\mathrm{d}x} &= -\frac{q}{2bt_c^3}(L-x)x, \\ C_{v\psi_0}\frac{\mathrm{d}^3 v}{\mathrm{d}x^3} - C_{\psi_0\psi_0}\frac{\mathrm{d}^2\psi_0}{\mathrm{d}x^2} + G_c\frac{\psi_0(x,t)}{t_c^2} &= 0. \end{aligned} \tag{3.1}$$

This system, after simple transformation, is reduced to one differential equation

$$\frac{\mathrm{d}^2\psi_0}{\mathrm{d}x^2} - k^2\frac{\psi_0(x)}{t_c^2} = -k^2\frac{C_{v\psi_0}}{C_{vv}}\frac{q}{2G_c b t_c^3}(L-2x), \tag{3.2}$$

where

$$k = \sqrt{\frac{G_c C_{vv}}{C_{vv}C_{\psi_0\psi_0} - C_{v\psi_0}^2}}$$

is dimensionless coefficient.

The solution of this equation is as follows

$$\psi_0(x) = C_1 \sinh\left(k\frac{x}{t_c}\right) + C_2\cosh\left(k\frac{x}{t_c}\right) + \frac{C_{v\psi_0}}{C_{vv}}\frac{q}{2G_c b t_c}\left(L-2x\right). \tag{3.3}$$

The two boundary conditions of this function are:

$$x = 0, \qquad \left.\frac{\mathrm{d}\psi_0}{\mathrm{d}x}\right|_0 = 0, \qquad x = \frac{L}{2}, \qquad \psi_0\left(\frac{L}{2}\right) = 0. \tag{3.4}$$

Taking into account these conditions the integration constants are determined

$$C_1 = \frac{1}{k}\frac{C_{v\psi_0}}{C_{vv}}\frac{q}{G_c b} \quad \text{and} \quad C_2 = -\frac{1}{k}\tanh\left(\frac{1}{2}k\lambda\right)\frac{C_{v\psi_0}}{C_{vv}}\frac{q}{G_c b}, \tag{3.5}$$

where $\lambda = L/t_c$ is relative length of the beam.

Thus, the dimensionless function of the shear effect

$$\psi_0(x) = \left\{\frac{2}{k}\left[\sinh\left(k\frac{x}{t_c}\right) - \tanh\left(\frac{1}{2}k\lambda\right)\cosh\left(k\frac{x}{t_c}\right)\right] + \lambda\left(1-2\frac{x}{L}\right)\right\}\frac{C_{v\psi_0}}{C_{vv}}\frac{q}{2G_c b}. \tag{3.6}$$

Substituting this function into the first equation of the system (3.1), integrating twice and considering two boundary conditions:

$$x = \frac{L}{2}, \qquad \left.\frac{\mathrm{d}v}{\mathrm{d}x}\right|_{L/2} = 0, \qquad x = 0, \qquad v(0) = 0, \tag{3.7}$$

one obtains the deflection of the beam middle

$$v_m = v\left(\frac{L}{2}, \eta_0\right) = \widetilde{v}_m\left(\eta_0\right)\cdot\frac{qL}{E_c b}, \tag{3.8}$$

where the dimensionless deflection of the beam middle

$$\widetilde{v}_m(\eta_0) = \lambda \left\{ \frac{5}{384}\lambda^2 + \left[\frac{1}{8} - \frac{1}{(k\lambda)^2} \left(1 - \frac{1}{\cosh(k\lambda/2)} \right) \right] \frac{C_{v\psi_0}^2}{G_c C_{vv}} \right\} \frac{E_c}{C_{vv}}. \tag{3.9}$$

Therefore, taking into account the expression (2.22), the dimensionless maximal deflection of the beam

$$\widetilde{v}_{\max} = \max_{\eta_0} \{\widetilde{v}_m(\eta_0)\}. \tag{3.10}$$

The detailed calculations of the maximal deflections are carried out for exemplary unsymmetrical structures of sandwich beams and reported in Table 1.

Table 1. Specification of the data of the exemplary beams.

Beam type	B-1	B-2	B-3	B-4
E_{f1} [GPa]	200	200	200	200
ρ_{f1} [kg/m^3]	7850	7850	7850	7850
E_{f2} [GPa]	75	75	200	200
ρ_{f2} [kg/m^3]	2710	2710	7850	7850
E_c [GPa]	1	1	1	1
ρ_c [kg/m^3]	250	250	250	250
t_{f1} [mm]	2	1	1	2
t_{f2} [mm]	1	1	1	1
t_c [mm]	80	80	80	80

The relative length of the beam takes the following values: $\lambda = 5$, 10, 15, 20, 25. The values of dimensionless parameter η_0 and maximal deflection $\widetilde{v}_{\max}$ of the beams calculated based on (3.10) are specified in Tables 2–5.

However, taking into account the simplified expression (2.21) determining position of the neutral axis without shear effect, one obtains $\eta_0 = 0.30096$ and the values of the maximal deflection $\widetilde{v}_{\max}$ identical as in Table 2. Maximum difference between the neutral axis positions determined from (3.10) and (2.21) amounts to 3% in case of the shortest beam ($\lambda = 5$). The difference decreases

Table 2. The values of the parameter η_0 and maximal deflection $\widetilde{v}_{\max}$ – the beam B-1.

λ	5	10	15	20	25
η_0	0.30968	0.30306	0.30189	0.30148	0.30129
$\widetilde{v}_{\max}$	3.229	16.137	48.407	109.719	209.752

with growing beam length. Hence, the simplified expression (2.21) is sufficient for determination of the neutral axis position of unsymmetrical sandwich beams.

The value of the dimensionless parameter defining the neutral axis position calculated based on (2.21) for the sandwich beam is $\eta_0 = 0.17826$. Hence, the values of maximal deflection $\widetilde{v}_{\max}$ calculated using this value are identical as in Table 3. Maximum difference between the neutral axis positions determined from (3.10) and (2.21) is below 2% in case of the shortest beam ($\lambda = 5$). The difference significantly decreases with growing beam length.

Table 3. The values of the parameter η_0 and maximal deflection $\widetilde{v}_{\max}$ – the beam B-2.

λ	5	10	15	20	25
η_0	0.18126	0.17879	0.17847	0.17838	0.17833
$\widetilde{v}_{\max}$	3.606	19.086	58.283	133.062	255.283

Table 4. The values of the dimensionless maximal deflection $\widetilde{v}_{\max}$ – the beam B-3.

λ	5	10	15	20	25
$\widetilde{v}_{\max}$	2.824	12.810	37.105	82.865	157.245

Since the B-3 beam is a symmetrical structure, the neutral axis position determined from (3.10) and (2.21) is $\eta_0 = 0$.

The value of the dimensionless parameter defining the position of the neutral axis calculated on the base of (2.21) for the sandwich beam is $\eta_0 = 0.15257$. The values of the maximal deflection $\widetilde{v}_{\max}$ calculated with the use of his value are identical as in the Table 5. Maximum difference between the neutral axis positions determined from (3.10) and (2.21) exceeds 7% in case of the shortest beam ($\lambda = 5$). The difference decreases with growing beam length, taking 0.3% for $\lambda = 25$.

Table 5. The values of the parameter η_0 and maximal deflection $\widetilde{v}_{\max}$ the beam B-4.

λ	5	10	15	20	25
η_0	0.16374	0.15519	0.15371	0.15322	0.15299
$\widetilde{v}_{\max}$	2.500	10.308	28.732	63.081	118.662

Graphical illustration of the neutral axis position calculated based on (3.10) and (2.21) for the exemplary beams (B-1, B-2, and B-4) is shown in Figs 4–6.

Taking into account that maximal deflections $\widetilde{v}_{\max}$ obtained from the iterative procedure (3.10) and based on previously determined η_0 (2.21) are identical, further research of critical force and natural frequencies are carried out only with the second approach.

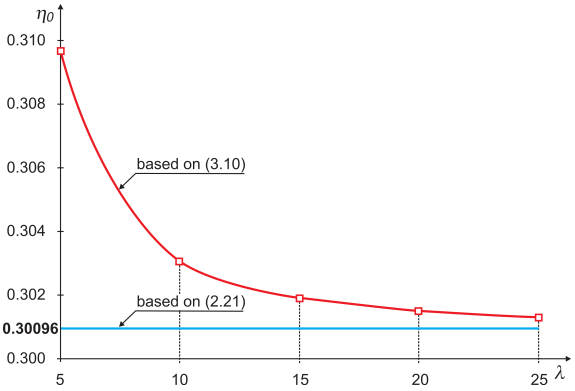

FIG. 4. Positions of the neutral axes η_0 calculated for the B-1 beam.

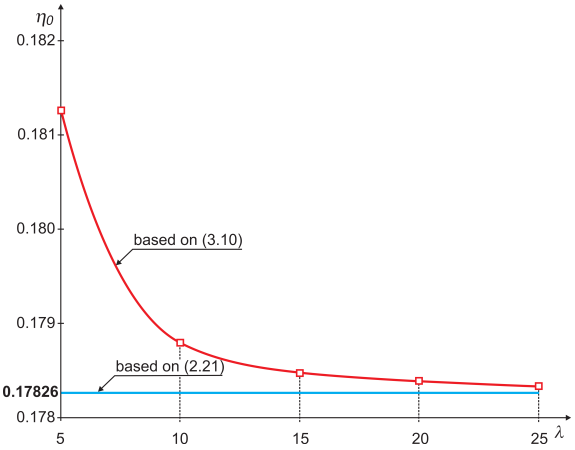

FIG. 5. Positions of the neutral axes η_0 calculated for the B-2 beam.

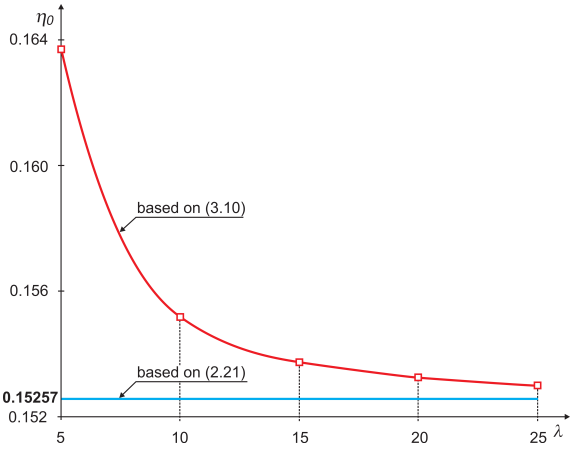

FIG. 6. Positions of the neutral axes η_0 calculated for the B-4 beam.

3.2. Buckling of the beam – static problem

The system of two equations of equilibrium (2.18) and (2.16) for buckling of the sandwich beam is in the following form

$$
\begin{aligned}
&C_{vv}\frac{\mathrm{d}^2 v}{\mathrm{d}x^2} - C_{v\psi_0}\frac{\mathrm{d}\psi_0}{\mathrm{d}x} = -\frac{F_0}{bt_c^3}v(x),\\
&C_{v\psi_0}\frac{\mathrm{d}^3 v}{\mathrm{d}x^3} - C_{\psi_0\psi_0}\frac{\mathrm{d}^2\psi_0}{\mathrm{d}x^2} + G_c\frac{\psi_0(x,t)}{t_c^2} = 0.
\end{aligned}
\tag{3.11}
$$

This system is approximately solved with the use of two assumed functions

$$
v(x) = v_a \sin\left(\pi\frac{x}{L}\right), \qquad \psi_0(x,t) = \psi_a \cos\left(\pi\frac{x}{L}\right),
\tag{3.12}
$$

where v_a, ψ_a – parameters of the functions.

These functions satisfy the conditions of simply supported beam. Substitution of these functions (3.12) into the equations (3.11) gives the homogeneous system of algebraic equations:

$$
\begin{aligned}
&\left[\left(\frac{\pi}{L}\right)^2 C_{vv} - \frac{F_0}{bt_c^3}\right] v_a - \frac{\pi}{L}C_{v\psi_0}\psi_a = 0,\\
&\left(\frac{\pi}{L}\right)^3 C_{v\psi_0} v_a - \left[\left(\frac{\pi}{L}\right)^2 C_{\psi_0\psi_0} + \frac{G_c}{t_c^2}\right]\psi_a = 0,
\end{aligned}
\tag{3.13}
$$

from which

$$
F_{0,CR} = \widetilde{F}_{0,CR}\cdot E_c b t_c.
\tag{3.14}
$$

The dimensionless critical force

$$
\widetilde{F}_{0,CR} = \left(\frac{\pi}{\lambda}\right)^2 (1-\alpha_{se})\,\frac{C_{vv}}{E_c},
\tag{3.15}
$$

and dimensionless parameter of shear effect

$$
\alpha_{se} = \frac{\pi^2 C_{v\psi_0}^2}{C_{vv}\left(\pi^2 C_{\psi_0\psi_0} + \lambda^2 G_c\right)}.
\tag{3.16}
$$

The detailed calculations of the critical force are carried out for identical exemplary structures of sandwich beams as for bending (B-1, B-2, B-3, B-4). The values of dimensionless parameter η_0 calculation on the basis of the expression (2.21) are specified in Table 6.

The values of the dimensionless critical force $\widetilde{F}_{0,CR}$ (3.15) for example beams (B-1, B-2, B-3, B-4) are specified in Table 7.

Table 6. The values of dimensionless parameter η_0 (**??**) for the beams B-1–B-4.

Beam	B-1	B-2	B-3	B-4
η_0	0.30096	0.17826	0	0.15257

Table 7. The values of the dimensionless critical force $\widetilde{F}_{0,CR}$ – the beams B-1–B-4.

λ	15	20	25	30	35
B-1	0.03971	0.02330	0.01530	0.01076	0.00796
B-2	0.03299	0.01929	0.01257	0.008821	0.006520
B-3	0.05176	0.03095	0.02040	0.01440	0.01069
B-4	0.06677	0.04063	0.02702	0.01918	0.01428

3.3. Free vibration of the beam – dynamic problem

The system of two differential equations of motion (2.15) and (2.16) for the free vibration problem of the simply supported sandwich beam is in the following form

$$\begin{aligned} &\rho_b \frac{\partial^2 v}{\partial t^2} + t_c^2 \left(C_{vv} \frac{\partial^4 v}{\partial x^4} - C_{v\psi_0} \frac{\partial^3 \psi_0}{\partial x^3} \right) = 0, \\ &C_{v\psi_0} \frac{\partial^3 v}{\partial x^3} - C_{\psi_0\psi_0} \frac{\partial^2 \psi_0}{\partial x^2} + G_c \frac{\psi_0(x,t)}{t_c^2} = 0. \end{aligned} \tag{3.17}$$

This system is approximately solved with the use of two assumed functions

$$v(x,t) = v_a(t) \sin\left(\pi \frac{x}{L}\right), \qquad \psi(x,t) = \psi_a(t) \cos\left(\pi \frac{x}{L}\right), \tag{3.18}$$

where $v_a(t)$, $\psi_a(t)$ are functions of time t.

Substitution of these functions (3.18) into the equations (3.17) gives two following equations:

$$\begin{aligned} &\rho_b \frac{d^2 v_a}{dt^2} + t_c^2 \left(\frac{\pi}{L}\right)^4 C_{vv} v_a(t) - t_c^2 \left(\frac{\pi}{L}\right)^3 C_{v\psi_0} \psi_a(t) = 0, \\ &\left(\frac{\pi}{L}\right)^3 C_{v\psi_0} v_a(t) - \left(\frac{\pi}{L}\right)^2 \left[C_{\psi_0\psi_0} + \left(\frac{\lambda}{\pi}\right)^2 G_c \right] \psi_a(t) = 0. \end{aligned} \tag{3.19}$$

From which, after simple transformation, the function

$$\psi_0(t) = \frac{\pi^2 C_{v\psi_0}}{\pi^2 C_{\psi_0\psi_0} + \lambda^2 G_c} \frac{\pi}{L} \cdot v_a(t), \tag{3.20}$$

and the differential equation of free linear vibration of the unsymmetrical sandwich beam

$$\rho_b \frac{\mathrm{d}^2 v_a}{\mathrm{d}t^2} + \left(\frac{\pi}{\lambda}\right)^2 C_{vv}\,(1-\alpha_{se}) \left(\frac{\pi}{L}\right)^2 v_a(t) = 0, \tag{3.21}$$

where α_{se} is dimensionless parameter of shear effect (3.16).

The equation is approximately solved with the use of the assumed function

$$v_a(t) = v_a \sin(\omega t), \tag{3.22}$$

where v_a – amplitude of the flexural vibration, ω – fundamental natural frequency.

Substituting this function into the equation (3.18), after simple transformation, one obtains the fundamental natural frequency

$$\omega = \left(\frac{\pi}{\lambda}\right)^2 \sqrt{\frac{C_{vv}\,(1-\alpha_{se})}{\rho_b t_c^2}}. \tag{3.23}$$

Taking into account the expression for the dimensionless critical force (3.15), the above expression for fundamental natural frequency takes the following form

$$\omega = \frac{\pi}{\lambda} \sqrt{\frac{E_c}{\rho_b t_c^2} \widetilde{F}_{0,CR}}. \tag{3.24}$$

The detailed calculations of the fundamental natural frequency ω (3.23) is carried out for identical example structures of sandwich beams as for bending or buckling (B-1, B-2, B-3, B-4). The values of parameter η_0 is calculated on the base of the expression (2.21).

The values of the fundamental natural frequency ω [1/s] (3.23) for example beams (B-1, B-2, B-3, B-4) are specified in Table 8.

Table 8. The values of the fundamental natural frequency ω [1/s] – the beams B-1–B-4.

λ	10	15	20	25	30
B-1	1595	752.9	433.3	280.4	195.9
B-2	1645	769.4	441.2	285.0	198.9
B-3	1855	891.6	517.1	335.9	235.2
B-4	1871	916.9	536.4	350.0	245.7

The values of fundamental natural frequency ω and critical forces $\widetilde{F}_{0,CR}$ are coupled each with other, according to Mathieu equation.

4. Numerical calculations – FEM study

Numerical analysis of the unsymmetrical sandwich beams is carried out in parallel with ABAQUS and SolidWorks software systems. The doubled comparison of the numerical and analytical solutions improves reliability of the verification. The simulation assumed the same geometric parameters and mechanical properties as the ones used in the analytical calculations.

Taking into account symmetry of the structure the model is confined to a quarter of the whole beam (Fig. 7) and subjected to the boundary conditions simulating considered behaviour of the beam.

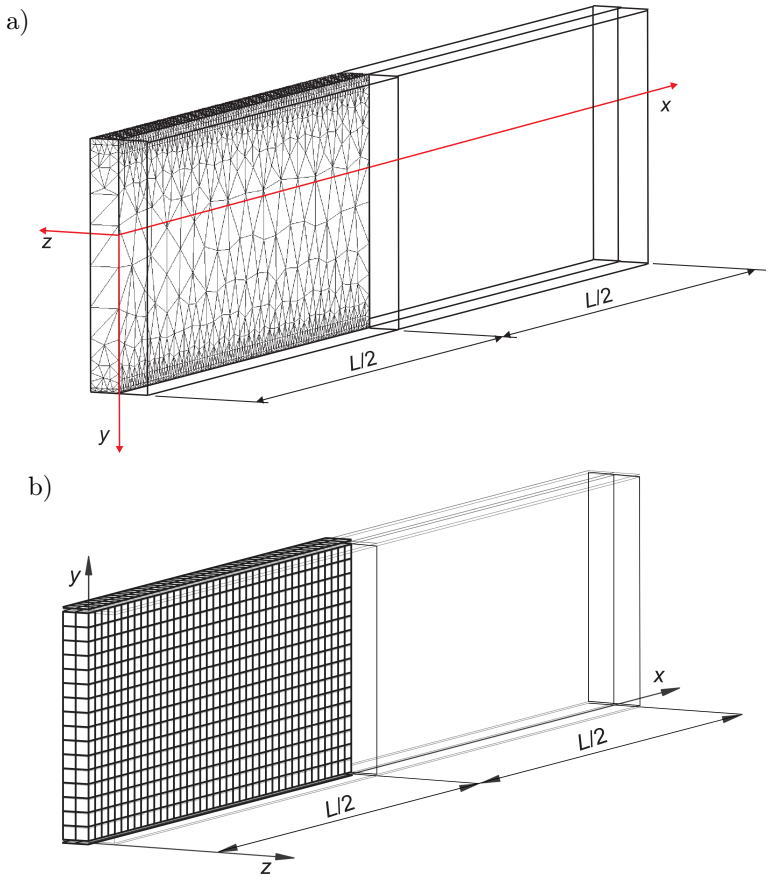

Fig. 7. Beam model adopted for purposes of FEM study:
a) Solid Works mesh, b) ABAQUS mesh.

a) SolidWorks model – the coordinate system is so situated that the longitudinal middle plane of the beam coincides with xy-plane. The x-axis is collinear with neutral axis of the beam, y-axis is downward directed. The

considered quarter of the beam is located at the area of positive z-values. The beam is modelled as a single part and divided into 3D tetrahedral finite elements with four Gauss points. Since the faces are thin as compared to the core, the mesh of elements is decidedly finer in the face areas than in the core.

b) ABAQUS model – the x-axis is collinear with symmetry axis of the bottom surface of the lower face of the beam, y-axis is upward directed. The considered quarter of the beam is located at the area of negative z-values. The beam model consists of three parts: the core is modelled as a solid divided into quadratic hexahedral elements, while both faces are shell structures built of quadratic quadrilateral elements. Particular parts are assembled with the "tie" constraints.

The following geometric conditions are adopted:

- for $x = 0$ a simple support at the beam wall coinciding with yz-plane – the $v(0)$ displacements in y direction are zero;
- for $x = L/2$ at the middle of the beam – the $u(L/2)$ displacements in x direction are zero;
- for $z = 0$, i.e. at the beam wall coinciding with xy-plane – the $w(0)$ displacements in z direction are zero.

The above boundary conditions assumed for purposes of the FEM model are equivalent to the case of simply supported beam. In case of SolidWorks approach the location of the coordinate system xyz corresponds to the one assumed in the analytical model. In ABAQUS approach the coordinate system differs from the one used for purposes of the analytical calculation (Fig. 7b), but the x-axes of both systems are of the same direction and sense. Nevertheless, it should be noticed that location of the coordinate system does not affect the results obtained from FEM computation, since the formulated boundary conditions are decisive for the results.

Numerical study of bending, buckling and free vibration is confined to the xy-plane, similarly as in case of the analytical approach.

4.1. Numerical FEM model – SolidWorks

The SolidWorks calculation has been carried out for the beams of rectangular cross-section with core depth $h = 80$ mm, width $b = 20$ mm, and length values $L = \lambda \cdot h$ ($400 \text{ mm} \leq L \leq 2800$ mm). Thickness values of the faces vary according to the beam variants B1–B4 defined before.

4.1.1. Bending of the beam, static problem – numerical FEM solution. The beam is subjected to uniformly distributed load of intensity q.

Results of the study, i.e. maximum deflection values, are specified in Table 9.

Table 9. The values of the dimensionless maximal deflection $\widetilde{v}_{\max}$ – the SolidWorks study.

λ	5	10	15	20	25
B-1	3.311	16.217	48.494	109.804	209.827
B-2	3.670	19.118	58.299	133.049	255.228
B-3	2.856	12.787	37.054	82.780	157.119
B-4	2.551	10.322	28.731	63.064	118.624

Relative difference values between analytical and FEM solutions (Tables 2–5 vs. Table 9) are below 2.5 per cent. The highest difference occurs for small relative length values λ. For greater λ values the difference decreases.

4.1.2. Buckling of the beam, static problem – numerical SolidWorks solution. The force causing buckling of the beam should be applied to its neutral axis (Table 6) located in the core that, first of all, would cause denting of the core. Therefore, proper forces are applied only to the faces, in the proportion guaranteeing the resultant coinciding with the neutral axis of the beam. Results of the study are critical force values specified in Table 10.

Table 10. The values of the dimensionless critical force $\widetilde{F}_{0,CR}$ – the FEM study.

λ	15	20	25	30	35
B-1	0.03925	0.02320	0.015210	0.01070	0.007929
B-2	0.03252	0.01909	0.01247	0.008764	0.006486
B-3	0.05119	0.03070	0.02028	0.01433	0.01064
B-4	0.06618	0.04036	0.02689	0.01910	0.01425

Relative difference values between analytical and FEM solutions (Table 7 vs. Table 10) are below 1.5 per cent.

4.1.3. Free vibration of the beam, dynamic problem – numerical SolidWorks solution. The SolidWorks simulation tool used to compute the free-vibration frequencies provides the angular frequencies ω of particular vibration modes. The adopted geometric conditions cause that the first vibration mode is identical to the buckling.

The values of fundamental natural frequency ω [1/s] for example beams (B-1, B-2, B-3, B-4) are specified in Table 11.

They perfectly comply with the results obtained analytically (Table 9 vs. Table 11). The difference does not exceed 0.5 per cent.

Table 11. The values of fundamental natural frequency ω [1/s] – the FEM study.

λ	10	15	20	25	30
B-1	1586	750.7	432.6	280.1	195.8
B-2	1638	767.7	440.6	284.7	198.8
B-3	1850	890.0	516.5	335.6	235.1
B-4	1865	915.1	535.7	349.7	245.5

4.2. Numerical FEM model – ABAQUS.

Numerical study with the help of ABAQUS software is carried out with the use of the same model of a quarter of the beam. The results of the study are presented in Tables 12–14.

Table 12. The values of the maximal deflection $\widetilde{v}_{\max}$ – the beams B-1–B-4.

λ	5	10	15	20	25
B-1	3.327	16.249	48.553	109.907	209.985
B-2	3.682	19.149	58.367	133.169	255.415
B-3	2.866	12.805	37.092	82.846	157.22
B-4	2.563	10.341	28.763	63.113	118.701

Relative difference values between analytical and FEM solutions (Tables 2–5 vs. Table 12) do not exceed 3 per cent. The highest difference occurs for small relative length values λ. For greater λ values the difference decreases.

Table 13. The values of the dimensionless critical force $\widetilde{F}_{0,CR}$ – the beams B-1–B-4.

λ	15	20	25	30	35
B-1	0.03896	0.02311	0.01517	0.01068	0.00792
B-2	0.03239	0.01906	0.01246	0.00876	0.00648
B-3	0.05078	0.03063	0.02026	0.01433	0.01064
B-4	0.06513	0.04022	0.02684	0.01908	0.01422

Relative difference values between analytical and FEM solutions (Table 7 vs. Table 13) are below 2.5 per cent.

Table 14. The values of the fundamental natural frequency ω [1/s] – the beams B-1–B-4.

λ	10	15	20	25	30
B-1	1585	750.5	432.5	280	195.7
B-2	1637	767.4	440.5	284.7	198.8
B-3	1849	889.6	516.4	335.5	235
B-4	1865	914.8	535.6	349.6	245.5

They perfectly comply with the results obtained analytically (Table 8 vs. Table 14). The difference does not exceed 0.5 per cent.

5. Conclusions

The values of deflection, critical load, and free-vibration frequencies depend on position of the neutral axis. Detailed study performed with iteration method (expressions (2.22), (2.23)) and with simplified approach (expression (2.21) gave the same position of the neutral axis.

The difference between the neutral axis locations determined based on maximization of maximal deflection (2.22) and approximate method (2.21) decreases for longer beams (i.e. for growing λ values – Figs 4–6). The effect of the above mentioned difference on maximum deflection values is insignificant. Moreover, in case of buckling and free vibration of longer beams this effect is negligible.

Based on comparison of the results obtained analytically and numerically with SolidWorks and ABAQUS software it may be noticed that the difference between them does not exceed 2.5 per cent.

References

1. Vinson J.R., *Sandwich structures*, Applied Mechanics Reviews, **54**(3): 201–214, 2001.
2. Carrera E., *Historical review of zig-zag theories for multilayers plates and shells*, Applied Mechanics Reviews, **56**(3): 287–308, 2003.
3. Frostig Y., Shenhar Y., *High-order bending of sandwich beams with a transversely flexible core and unsymmetrical laminated composite skins*, Composites Engineering, **5**(4): 405–414, 1995.
4. Icardi U., *Applications of Zig-Zag theories to sandwich beams*, Mechanics of Advanced Materials and Structures, **10**(1): 77–97, 2003.
5. Kim J., Swanson S.R., *Effect of unequal face thickness on load resistance of sandwich beams*, Journal of Sandwich Structures and Materials, **6**(2): 145–166, 2004.
6. Backstöm D., Nilsson A., *Modeling flexural vibration of a sandwich beam using modified fourth-order theory*, Journal of Sandwich Structures and Materials, **8**(6): 465–476, 2006.
7. Magnucka-Blandzi E., Magnucki K., *Effective design of a sandwich beam with metal foam core*, Thin-Walled Structures, **45**: 432–438, 2007.
8. Magnucka-Blandzi E., *Dynamic stability and static stress state of a sandwich beam with a metal foam core using three modified Timoshenko hypothesis*, Mechanics of Advanced Materials and Structures, **18**(2): 147–158, 2011.
9. Wang Z.D., Li Z.F., *Theoretical analysis of the deformation of SMP sandwich beam in flexure*, Archive of Applied Mechanics, **81**: 1667–1678, 2011.

10. Baba B.O., *Free vibration analysis of curved sandwich beams with face/core debond using theory and experiment*, Mechanics of Advanced Materials and Structures, **19**(5): 350–359, 2012.

11. Eltaher M.A., Alshorbagy A.E., Mahmoud F.F., *Determination of neutral axis position and its effect on neutral frequencies of functionally graded macro/nanobeams*, Composite Structures, **99**: 193–201, 2013.

12. Jasion P., Magnucki K., *Global buckling of a sandwich column with metal foam core*, Journal of Sandwich Structures and Materials, **15**(6): 718–732, 2013.

13. Magnucki K., Jasion P., Szyc W., Smyczyński M., *Strength and buckling of a sandwich beam with thin binding layers between faces and a metal foam core*, Steel and Composite Structures, **16**(3): 325–337, 2014.

14. Wu H., Kitipornchai S., Yang J., *Free vibration and buckling analysis of sandwich beams with functionally graded carbon nanotube-reinforced composite face sheets*, International Journal of Structural Stability and Dynamics, **15**(7): No. 1540011, 2015.

15. Filippi M., Carrera E., *Bending and vibrations analyses of laminated beams by using a zig-zag-layer-wise theory*, Composites Part B, **98**: 269–280, 2016.

16. Frostig Y., *Shear buckling of sandwich plates – Incompressible and compressible cores*, Composites Part B, **96**(1): 153–172, 2016.

17. Kim N-I., Lee J., *Geometrically nonlinear isogeometric analysis of functionally graded plates based on first-order shear deformation theory considering physical neutral surface*, Composite Structures, **153**: 804–814, 2016.

18. Chen D., Kitipornchai S., Yang J., *Nonlinear free vibration of shear deformable sandwich beam with a functionally graded porous core*, Thin-Walled Structures, **107**: 39–48, 2016.

19. Magnucka-Blandzi E., Rodak M., *Bending and buckling of a metal seven-layer beam with lengthwise corrugated main core – comparative analysis with sandwich beam*, Journal of Theoretical and Applied Mechanics, **55**(1): 41–53, 2017.

20. Magnucka-Blandzi E., *Bending and buckling of a metal seven-layer beam with crosswise corrugated main core – comparative analysis with sandwich beam*, Composite Structures, **183**(1): 35–41, 2018.

21. Sayyad A.S., Ghugal Y.M., *Bending, buckling and free vibration of laminated composite and sandwich beams: A critical review of literature*, Composite Structures, **171**: 486–504, 2017.

22. Yang Y., Pagani A., Carrera E., *Exact solutions for free vibration analysis of laminated, box and sandwich beams by refined layer-wise theory*, Composite Structures, **175**: 28–45, 2017.

23. Vo T.P., Thai H-T., Nguyen T-K., Lanc D., Karamanli A., *Flexural analysis of laminated composite and sandwich beams using a four-unknown shear and normal deformation theory*, Composite Structures, **176**: 388–397, 2017.

24. Zhen W., Yang C., Zhang H., Zheng X., *Stability of laminated composite and sandwich beams by a Reddy-type higher-order zig-zag theory*, Mechanics of Advanced Materials and Structures, (Published online: 12 Mar 2018).

25. Sayyad A.S., Ghugal Y.M., *Modeling and analysis of functionally graded sandwich beams: A review*, Mechanics of Advanced Materials and Structures, (Published online: 19 Mar 2018).

26. Magnucki K., *Bending of symmetrically sandwich beams and I-beams – Analytical study*, International Journal of Mechanical Science, **150**: 411–419, 2019.

Received January 2, 2019; accepted version May 7, 2019.